

Response to Reviewer 3 comments. R3 Comments normal font, *Responses in italics*

The paper represents a first attempt to use parflow to simulate continental scale hydrologic processes, demonstrating a methodology for using existing physical observations to generate a numerical simulation that results in a natural organization of stream networks and groundwater flow. Such an approach may also be of interest to the geomorphology and geochemistry communities. The manuscript should definitely be published in GMD.

We thank the reviewer both for their constructive comments and for recognizing the merits and novelty of this work.

The previous review comments reflect considerable differences of opinion regarding novelty and the conceptualization. Although the authors have done a commendable job in responding to these comments, one thing I suggest the authors consider is a more detailed statement, possibly at the end of the results/discussion regarding (a) how or could such simulations could be improved through better parameterization (for example better resolution in the depth of subsurface, fixing state boundaries, etc? There is a general statement at line 487 but thoughts on how to prioritize additional products would be useful. (b) Do the authors think the resolution (perhaps for surface water) and parameterization impacts any of the scaling results (for example around figure 10 and 11).

We agree with the reviewer that these are great points to add to the discussion. We have expanded the discussion regarding improved input datasets, increased resolution and the scaling results.

Line 17: “tools for” and “processes; however, “

Change made in the revised manuscript.

Line 19: need to be or can only be?

Changed to “only be” in revised manuscript.

Line 22: Why give the area twice? First time seems sufficient.

Second area removed.

Line 30: recommend removing the word novel – readers should decide for themselves.

“Novel” removed in revised manuscript.

Line 45: “bridge this gap” is rather informal. Suggest replacing this phrase.

Changed to ‘address this need’ in the revised manuscript.

Line 78: “groundwater-surface water”

Change made in the revised manuscript.

Line 97: “extent (i.e. continental scale)” (there is more than one continent).

Change made in the revised manuscript.

Line 98: missing space “(1 km)

Change made in the revised manuscript.

Line 134: define S_x , S_y ?

S_x and S_y now defined as the local topographic slope.

Line 166: “Physically this” – define “this” or delete.

Phrase “Physically this means that” deleted in revised manuscript.

Line 205: “functional relationships that impose”

Change made in the revised manuscript.

Line 208: This somewhat repeats what is stated at Line 162.

We feel the two are different enough and that this is an important point to bear repeating.

Line 221-237: missing spaces between values and units throughout: 102 m, 1 km, 100 m, 1 x 1 km, etc. please correct. This occurs throughout manuscript and some figures and should be corrected.

Changes made in the revised manuscript.

Line 229: It seems to me that several things are missing from the discussion. First, how is porosity specified? Second, at some point in the manuscript a discussion or acknowledgment regarding the bottom layer of the model relative to realistic physical conditions should be included. I am not familiar with the exact details or issues associated with the Gleeson et al. (2001) map, but the current simulation includes a

highly simplified treatment of the actual bottom boundary of the subsurface – namely the presence of low-porosity impermeable bedrock. I realize there is no other option than the assumption made, but if for example depth of regolith would improve the model considerably vs. not at all, that is important information to provide to the community.

Finally, it would be helpful to provide more information about the various products used here. I realize the references are included but for example, how is the soil conductivity in the two layers determined? Also, the basics of the Gleeson map construction.

The reviewer makes a good point here. We have added discussion on the need for deeper hydrogeologic data and more information regarding the process of assigning variables.

Figure 1: I did not find the description very clear relative to figure 1. What is plotted in (E)? Conductivity where? Below 2 m?

Figure 1 caption clarified to specify that the soil types are applied over the top 2 m and the hydraulic conductivity over the bottom 100 m.

Line 230: SSURGO – please define acronym.

Defined.

Line 237: minor point but S_x, S_y look lowercase in equation – are uppercase previously

This is just the formatting of S_x in the denominator of the equation, they are uppercase.

Line 239: tense “reduce”

Changes made in the revised manuscript.

Line 245:246: This is unclear – what kind of uncertainty? “As such” does not fit here.

Three types of uncertainty are described and “as such” removed.

Line 248: Interfaces “between” property values.

Changes made in the revised manuscript.

Line 257: possibly add “variability using best available data”. Also “impact of uncertain”

Change made in the revised manuscript.

Line 260-262: This statement is rather confusing. Please clarify. Was a new product created from another product or are the authors referring to an actual product? I also found it unclear exactly how unsaturated flow is handled- prescribed recharge? Please clarify with respect to equation 1.

This term was clarified both in the definition of qr in (1) and here.

Line 277: “far from being trivial”. What does this mean? Can authors be specific? Trivial is a relative word.

The phrase “far from being trivial” was replaced with “required significant computational resources” replacing one relative word with a somewhat less relative word. We feel that we are specific and quantitative regarding compute resources used for the simulation later in this paragraph.

Line 281: “still better than 60% efficiency”

Change made in the revised manuscript.

Line 293: “checked for plausibility against”? Do authors mean: “are compared to observations”?

Yes, change made.

Line 342: Change “while” to “although”

Change made in the revised manuscript.

Line 344: “in future work”?

Change made in the revised manuscript.

Line 347: What is a plausibility check? This is an evaluation against parameters that were not used to develop the simulations. Out of curiosity, are any of these datasets used to generate the P-ET or other “products” ?

Yes, basically that, and “no.” The sentence now reads: “Therefore, the purpose of these comparisons is to evaluate model behavior and physical processes against observations not used to generate input parameters.”

Line 354: Please clarify this statement –

Statement reworded for clarity.

Line 497: what does within “the confines of the numerical experiment” mean?

Phrase has been deleted.

1 A high resolution simulation of groundwater and surface water over most of the continental US
2 with the integrated hydrologic model ParFlow v3

3
4 Reed M Maxwell^{1*}, Laura E Condon¹, Stefan J Kollet²

5 ¹Hydrologic Science and Engineering Program, Integrated GroundWater Modeling Center, Department
6 of Geology and Geological Engineering, Colorado School of Mines, Golden, Colorado, USA

7 ²Centre for High-Performance Scientific Computing in Terrestrial Systems, Institute for Bio- and
8 Geosciences, Agrosphere (IBG-3), Research Centre Jülich, Jülich, DE

9
10 *correspondence to: Reed M Maxwell, rmaxwell@mines.edu

11 **Abstract**

12 Interactions between surface and groundwater systems are well-established theoretically and
13 observationally. While numerical models that solve both surface and subsurface flow equations
14 in a single framework (matrix) are increasingly being applied, computational limitations have
15 restricted their use to local and regional studies. Regional or watershed-scale simulations have
16 been effective tools ~~for~~ understanding hydrologic processes; however there are still many
17 questions, such as the adaptation of water resources to anthropogenic stressors and climate
18 variability, that ~~can only~~ be answered across large spatial extents at high resolution. In response
19 to this ‘grand challenge’ in hydrology, we present the results of a parallel, integrated hydrologic
20 model simulating surface and subsurface flow at high spatial resolution (1km) over much of
21 continental North America (~6,300,000 km²). These simulations provide integrated predictions
22 of hydrologic states and fluxes, namely water table depth and streamflow, at very large scale and
23 high resolution. The physics-based modeling approach used here requires limited
24 parameterizations and relies only on more fundamental inputs, such as topography,
25 hydrogeologic properties and climate forcing. Results are compared to observations and provide
26 mechanistic insight into hydrologic process interaction. This study demonstrates both the
27 feasibility of continental scale integrated models and their utility for improving our
28 understanding of large-scale hydrologic systems; the combination of high resolution and large
29 spatial extent facilitates ~~analysis~~ of scaling relationships using model outputs.
30

Reed Maxwell 3/4/2015 7:55 AM

Deleted: in

Reed Maxwell 3/4/2015 7:55 AM

Deleted: ,

Reed Maxwell 3/4/2015 7:55 AM

Deleted: need to

Reed Maxwell 3/4/2015 7:55 AM

Deleted: or 6.3M

Reed Maxwell 3/4/2015 7:55 AM

Deleted: novel

36 **Introduction**

37 There is growing evidence of feedbacks between groundwater, surface water and soil
38 moisture that moderate land-atmospheric energy exchanges, and impact weather and climate
39 (Maxwell et al. 2007; Anyah et al. 2008; Kollet and Maxwell 2008; Maxwell and Kollet 2008;
40 Jiang et al. 2009; Rihani et al. 2010; Maxwell et al. 2011; Williams and Maxwell 2011; Condon
41 et al. 2013; Taylor et al. 2013). While local observations and remote sensing can now detect
42 changes in the hydrologic cycle from small to very large spatial scales (e.g. Rodell et al. 2009),
43 theoretical approaches to connect and scale hydrologic states and fluxes from point
44 measurements to the continental scales are incomplete. In this work, we present integrated
45 modeling as one means to address this need, via numerical experiments.

46 Though introduced as a concept in the literature almost half a century ago (Freeze and
47 Harlan 1969), integrated hydrologic models that solve the surface and subsurface systems
48 simultaneously have only been a reality for about a decade (VanderKwaak and Loague 2001;
49 Jones et al. 2006; Kollet and Maxwell 2006). Since their implementation, integrated hydrologic
50 models have been successfully applied to a wide range of watershed-scale studies (see Table 1 in
51 Maxwell et al. 2014) successfully capturing observed surface and subsurface behavior (Qu and
52 Duffy 2007; Jones et al. 2008; Sudicky et al. 2008; Camporese et al. 2010; Shi et al. 2013),
53 diagnosing stream-aquifer and land-energy interactions (Maxwell et al. 2007; Kollet and
54 Maxwell 2008; Rihani et al. 2010; Condon et al. 2013; Camporese et al. 2014), and building our
55 understanding of the propagation of perturbations such as land-cover and anthropogenic climate
56 change throughout the hydrologic system (Maxwell and Kollet 2008; Goderniaux et al. 2009;
57 Sulis et al. 2012; Mikkelsen et al. 2013).

Reed Maxwell 3/4/2015 7:55 AM
Deleted: bridge
Reed Maxwell 3/4/2015 7:55 AM
Deleted: gap

60 Prior to this work, computational demands and data constraints have limited the
61 application of integrated models to regional domains. Advances in parallel solution techniques,
62 numerical solvers, supercomputer hardware, and additional data sources have only recently made
63 large-scale, high-resolution simulation of the terrestrial hydrologic cycle technically feasible
64 (Kollet et al. 2010; Maxwell 2013). As such, existing large scale studies of the subsurface have
65 focused on modeling groundwater independently (Fan et al. 2007; Miguez-Macho et al. 2007;
66 Fan et al. 2013) and classifying behavior with analytical functions (Gleeson et al. 2011).
67 Similarly, continental scale modeling of surface water has utilized tools with simplified
68 groundwater systems that do not capture lateral groundwater flow and model catchments as
69 isolated systems (Maurer et al. 2002; Döll et al. 2012; Xia et al. 2012), despite the fact that
70 lateral flow of groundwater has been shown to be important across scales (Krakauer et al. 2014).
71 While much has been learned from previous studies, the focus on isolated components within
72 what we know to be an interconnected hydrologic system is a limitation that can only be
73 addressed with an integrated approach.

74 The importance of groundwater-surface water interactions in governing scaling behavior
75 of surface and subsurface flow from headwaters to the continent has yet to be fully characterized.
76 Indeed, one of the purposes for building an integrated model is to better understand and predict
77 the nature of hydrologic connections across scales and throughout a wide array of physical and
78 climate settings. Arguably, this is not possible utilizing observations, because of data scarcity
79 and the challenges observing 3D groundwater flow across a wide range of scales. For example,
80 the scaling behavior of river networks is well known (Rodriguez-Iturbe and Rinaldo 2001), yet
81 open questions remain about the quantity, movement, travel time, and spatial and temporal
82 scaling of groundwater and surface water at the continental scale. Exchange processes and flow

Reed Maxwell 3/4/2015 7:55 AM

Deleted:

84 near the land surface are strongly non-linear, and heterogeneity in hydraulic properties exist at all
85 spatial scales. As such, a formal framework for connecting scales in hydrology (Wood 2009)
86 needs to account for changes in surface water and groundwater flow from the headwaters to the
87 mouth of continental river basins. We propose that integrated, physics-based hydrologic models
88 are a tool for providing this understanding, solving fundamental non-linear flow equations at
89 high spatial resolution while *numerically* scaling these physical processes up to a large spatial
90 extent (i.e. continental scale).

91 In this study, we simulate surface and subsurface flow at high spatial resolution (1 km)
92 over much of continental North America (6.3M km²), which is itself considered a grand
93 challenge in hydrology (e.g. Wood et al. 2011; Gleeson and Cardiff 2014). The domain is
94 constructed entirely of available datasets including topography, soil texture and hydrogeology
95 This simulation solves surface and subsurface flow simultaneously and takes full advantage of
96 massively parallel, high-performance computing. The results presented here should be viewed as
97 a sophisticated numerical experiment, designed to diagnose physical behavior and evaluate
98 scaling relationships. While this is not a calibrated model that is intended to match observations
99 perfectly, we do verify that behavior is realistic by comparing to both groundwater and surface
100 water observations.

101 The paper is organized as follows: first a brief description of the model equations are
102 provided including a description of the input variables and observational datasets used for model
103 comparison; next model simulations are compared to observations in a number of ways, and then
104 used to understand hydrodynamic characteristics and to describe scaling.

105

106

Reed Maxwell 3/4/2015 7:55 AM

Deleted: the continent.

Reed Maxwell 3/4/2015 7:55 AM

Deleted: 1km

109 **Methods**

110 The model was constructed using the integrated simulation platform ParFlow (Ashby and
111 Falgout 1996; Jones and Woodward 2001; Kollet and Maxwell 2006) utilizing the terrain
112 following grid capability (Maxwell 2013). ParFlow is a physically based model that solves both
113 the surface and subsurface systems simultaneously. In the subsurface ParFlow solves the mixed
114 form of Richards' equation for variably saturated flow (Richards 1931) in three spatial
115 dimensions given as:

$$116 \quad S_s S_w(h) \frac{\partial h}{\partial t} + \phi S_w(h) \frac{\partial S_w(h)}{\partial t} = \nabla \cdot \mathbf{q} + q_r(x, z) \quad (1)$$

117 where the flux term \mathbf{q} [LT^{-1}] is based on Darcy's law:

$$118 \quad \mathbf{q} = -\mathbf{K}_s(\mathbf{x}) k_r(h) [\nabla(h+z) \cos \theta_x + \sin \theta_x] \quad (2)$$

119 In these expressions, h is the pressure head [L]; z is the elevation with the z -axis specified as
120 upward [L]; $\mathbf{K}_s(\mathbf{x})$ is the saturated hydraulic conductivity tensor [LT^{-1}]; k_r is the relative
121 permeability [-]; S_s is the specific storage [L^{-1}]; ϕ is the porosity [-]; S_w is the relative saturation [-
122]; q_r is a general source/sink term that represents transpiration, wells, and other fluxes including
123 the potential recharge flux, which is enforced at the ground surface [T^{-1}]; and θ [-] is the local
124 angle of topographic slope, S_x and S_y , in the x and y directions and may be written as
125 $\theta_x = \tan^{-1} S_x$ and $\theta_y = \tan^{-1} S_y$. Note that we assume that density and viscosity are both
126 constant, although ParFlow can simulate density and viscosity-dependent flow (Kollet et al.
127 2009). The van Genuchten (1980) relationships are used to describe the relative saturation and
128 permeability functions ($S_w(h)$ and $k_r(h)$ respectively). These functions are highly nonlinear and
129 characterize changes in saturation and permeability with pressure.

130 Overland flow is represented in ParFlow by the two-dimensional kinematic wave
131 equation resulting from application of continuity conditions for pressure and flux (Kollet and
132 Maxwell 2006):

$$133 \mathbf{k} \cdot (-\mathbf{K}_s(\mathbf{x})k_r(h) \cdot \nabla(h+z)) = \frac{\partial \|h,0\|}{\partial t} - \nabla \cdot \|h,0\| \mathbf{v}_{sw} + \lambda q_r(\mathbf{x}) \quad (3)$$

134 In this equation \mathbf{v}_{sw} is the two-dimensional, depth-averaged surface water velocity [LT^{-1}] given
135 by Manning's equation; h is the surface ponding depth [L] the same h as is shown in Equation 1.
136 Note that $\|h,0\|$ indicates the greater value of the two quantities in Equation 3. This means that
137 if $h < 0$ the left hand side of this equation represents vertical fluxes (e.g. in/exfiltration) across
138 the land surface boundary and is equal to $q_r(\mathbf{x})$ and a general source/sink (e.g. rainfall, ET) rate
139 [LT^{-1}] with λ being a constant equal to the inverse of the vertical grid spacing [L^{-1}]. This term is
140 then entirely equivalent to the source/sink term shown in Equation 1 at the ground surface where
141 \mathbf{k} is the unit vector in the vertical, again defining positive upward coordinates. If $h > 0$ then the
142 terms on the right hand side of Equation 3 are active water that is routed according to surface
143 topography (Kollet and Maxwell 2006).

144 The nonlinear, coupled equations of surface and subsurface flow presented above are
145 solved in a fully-implicit manner using a parallel Newton-Krylov approach (Jones and
146 Woodward 2001; Kollet and Maxwell 2006; Maxwell 2013). Utilizing a globally-implicit
147 solution allows for interactions between the surface and subsurface flow system to be explicitly
148 resolved. While this yields a very challenging computational problem, ParFlow is able to solve
149 large complex systems by utilizing a multigrid preconditioner (Osei-Kuffuor et al. ; Ashby and
150 Falgout 1996) and taking advantage of highly scaled parallel efficiency out to more than $1.6 \times$
151 10^4 processors (Kollet et al. 2010; Maxwell 2013).

152 ParFlow solves saturated subsurface flow (i.e. groundwater), unsaturated subsurface flow
153 (i.e. the vadose zone) and surface flow (i.e. streamflow) in a continuum approach within a single
154 matrix. Thus, complete non-linear interactions between all system components are simulated
155 without *a priori* specification of what types of flow occur in any given portion of the grid.
156 Streams form purely based on hydrodynamic principles governed by recharge, topography,
157 hydraulic conductivity and flow parameters, when water is ponded due to either excess
158 infiltration (surface fluxes exceed the infiltration capacity, e.g. Horton 1933) or excess saturation
159 (subsurface exfiltration to the surface system, e.g. Dunne 1983) for further discussion see Kirkby
160 (1988) and Beven (2004) for example. Groundwater converges in topographic depressions and
161 unsaturated zones may be shallow or deep depending upon recharge and lateral flows.

162 The physically based approach used by ParFlow is similar to other integrated hydrologic
163 models such as Hydrogeosphere (Therrien et al. 2012), PIHM (Kumar et al. 2009) and CATHY
164 (Camporese et al. 2010). This is a distinct contrast to more conceptually-based models that may
165 not simulate lateral groundwater flow or simplify the solution of surface and subsurface flow by
166 defining regions of groundwater or the stream-network prior to the simulation. In such models,
167 groundwater surface water interactions are often captured as one-way exchanges (i.e. surface
168 water loss to groundwater) or parameterized with simple relationships (i.e. functional
169 relationships that impose the relationship between stream head and baseflow). The integrated
170 approach used by ParFlow eliminates the need for such assumptions and allows the
171 interconnected groundwater surface water systems to evolve dynamically based only on the
172 governing equations and the properties of the physical system. The approach used here requires
173 robust numerical solvers (Maxwell 2013; Osei-Kuffuor et al. 2014) and exploits high-
174 performance computing (Kollet et al. 2010) to achieve high resolution, large extent simulations.

Reed Maxwell 3/4/2015 7:55 AM
Deleted: Physically this means that

Reed Maxwell 3/4/2015 7:55 AM
Formatted: Font:Times New Roman

Reed Maxwell 3/4/2015 7:55 AM
Formatted: Font:Times New Roman

Reed Maxwell 3/4/2015 7:55 AM
Formatted: Font:Times New Roman

Reed Maxwell 3/4/2015 7:55 AM
Deleted: to

Reed Maxwell 3/4/2015 7:55 AM
Formatted: Font:Times New Roman

Reed Maxwell 3/4/2015 7:55 AM
Deleted: [1]

Reed Maxwell 3/4/2015 7:55 AM
Formatted: Font:Times New Roman

179 Domain Setup

180 In this study, the model and numerical experiment was directed at the Continental US
181 (CONUS) using the terrain following grid framework (Maxwell 2013) for a total thickness of
182 102m over 5 model layers. The model was implemented with a lateral resolution of 1 km, with
183 $n_x=3342$, $n_y=1888$ and five vertical layers with 0.1, 0.3, 0.6, 1.0 and 100 m discretization for a
184 total model dimensions of 3,342 by 1,888 by 0.102 km and 31,548,480 total compute cells. The
185 model domain and input data sets are shown in Figure 1. All model inputs were re-projected to
186 have an equal cell-size of 1 x 1 km, as shown in Figure 1. Topographic slopes (S_x and S_y) were
187 calculated from the Hydrosheds digital elevation model (Figure 1b) and were processed using the
188 r.watershed package in the GRASS GIS platform. Surface roughness values were constant 10^{-5}
189 [$\text{h m}^{-1/3}$] outside of the channels and varied within the channel as a function of average watershed
190 slope. Over the top 2 m of the domain, hydraulic properties from soil texture information of the
191 Soil Survey Geographic Database (SSURGO) were applied and soil properties were obtained
192 from Schaap and Leij (1998). Note that two sets of soil categories were available. The upper
193 horizon was applied over the top 1m (the top three model layers) and the bottom one over the
194 next 1 m (the fourth model layer). These soil types were mapped to their corresponding category
195 in the property database and those values were used in the model simulation (e.g. saturated
196 hydraulic conductivity, van Genuchten relationships). Figures 1a and c show the top and bottom
197 soil layers of the model. The deeper subsurface (i.e. below 2 m) was constructed from a global
198 permeability map developed by Gleeson et al. (2011). These values (Gleeson et al. 2011) were
199 adjusted to reduce variance (Condon and Maxwell 2013; Condon and Maxwell 2014) and to
200 reflect changes in topography using the e-folding relationship empirically-derived in (Fan et al.

201 2007): $\alpha = e^{-\frac{50}{r}}$ where $f = \frac{a}{(1+b*\sqrt{S_x^2+S_y^2})}$. For this analysis $a=20$, $b=125$ and the value of 50

Reed Maxwell 3/4/2015 7:55 AM

Deleted: 1km

Reed Maxwell 3/4/2015 7:55 AM

Deleted: 100m

Reed Maxwell 3/4/2015 7:55 AM

Deleted: 1x1km

Reed Maxwell 3/4/2015 7:55 AM

Formatted: Superscript

Reed Maxwell 3/4/2015 7:55 AM

Deleted: 2m

Reed Maxwell 3/4/2015 7:55 AM

Deleted: .

Reed Maxwell 3/4/2015 7:55 AM

Deleted: 1m

Reed Maxwell 3/4/2015 7:55 AM

Deleted: 2m

209 [m] was chosen to reflect the midpoint of the deeper geologic layer in the model. Larger values
210 of α ~~reduce~~ the hydraulic conductivity categorically, that is by decreasing the hydraulic
211 conductivity indicator values in regions of steeper slope. Figure 1e maps the final conductivity
212 values used for simulation. ~~Below the deeper geologic layer, the presence of impermeable~~
213 ~~bedrock was assumed. This assumption oversimplifies regions that have weathered or fractured~~
214 ~~systems that contribute to regional flow and aquifer systems deeper than 100 m. These~~
215 ~~assumptions are necessitated by lack of data at this scale, not limitations of the model simulation.~~
216 Note that this complex subsurface dataset is assembled from many sources and is subject to
217 uncertainty: ~~heterogeneity within the defined geologic types, uncertainty about the breaks~~
218 ~~between geologic types and parameter values assigned to these types. There~~ are breaks across
219 dataset boundaries, commonly at State or Province and International political delineations. The
220 fidelity and resolution of the source information used to formulate this dataset also changes
221 ~~between~~ these boundaries yielding some interfaces in property values.

222 All input datasets are a work in progress and should be continually improved. However,
223 we feel it is important to continue numerical experiments with the data that is currently available,
224 while keeping in mind the limitations associated with every model input. Shortcomings in
225 hydrogeological data sets reflect the lack of detailed unified hydrogeological information that
226 can be applied in high resolution continental models. This constitutes a significant source of
227 uncertainty, which needs to be assessed, quantified and ultimately reduced in order to arrive at
228 precise predictions. Still, it should be noted that the purpose of this work is to demonstrate the
229 feasibility of integrated modeling to explicitly represent processes across many scales of spatial
230 variability ~~using best available data~~. By focusing on large-scale behaviors and relationships we
231 limit the impact ~~of~~ uncertain inputs.

Reed Maxwell 3/4/2015 7:55 AM

Deleted: reduced

Reed Maxwell 3/4/2015 7:55 AM

Deleted: . As such there

Reed Maxwell 3/4/2015 7:55 AM

Deleted: across

Reed Maxwell 3/4/2015 7:55 AM

Deleted: .

236 No-flow boundary conditions were imposed on all sides of the model except the land
237 surface, where the free-surface overland flow boundary condition was applied. For the surface
238 flux, a Precipitation-Evapotranspiration (P-E, or potential recharge) field, shown in figure 1d,
239 was derived from products developed by Maurer et al. (2002). They developed a gridded
240 precipitation field from observations and simulated evaporation and transpiration fluxes using
241 the VIC model. We calculate the average difference between the two from 1950-2000 and apply
242 all positive values as potential recharge (P-E) (negative values were set to zero). The model was
243 initialized dry and the P-E forcing was applied continuously at the land surface upper boundary
244 (q_r in equation 1) until the balance of water (difference between total outflow and P-E) was less
245 than 3% of storage. For all simulations a nonlinear tolerance of 10^{-5} and a linear tolerance of 10^{-10}
246 were used to ensure proper model convergence.

247 While this study employs state of the art modeling techniques, it is important to note that
248 the numerical simulation of this problem required significant computational resources.
249 Simulations were split over 128 divisions in the x -direction and 128 in the y -direction and run on
250 16,384 compute-cores of an IBM BG/Q supercomputer (JUQUEEN) located at the Jülich
251 Supercomputing Centre, Germany. These processor splits resulted in approximately 2,000
252 unknowns per compute core; a relatively small number, yet ParFlow's scaling was still better
253 than 60% efficiency due to the non-symmetric preconditioner used (Maxwell 2013). The reason
254 for this is the special architecture of JUQUEEN with only 256MB of memory per core and
255 relatively slow clock rate. Additionally, code performance was improved using efficient
256 preconditioning of the linear system (Osei-Kuffuor et al.). The steady-state flow field was
257 accomplished over several steps. Artificial dampening was applied to the overland flow
258 equations early in the simulation during water table equilibration. Dampening was subsequently

Reed Maxwell 3/4/2015 7:55 AM

Deleted: product

Reed Maxwell 3/4/2015 7:55 AM

Deleted: combination of

Reed Maxwell 3/4/2015 7:55 AM

Deleted: model-

Reed Maxwell 3/4/2015 7:55 AM

Deleted: for a product very similar

Reed Maxwell 3/4/2015 7:55 AM

Deleted: Maurer et al. (2002), shown in Figure 1d.

Reed Maxwell 3/4/2015 7:55 AM

Deleted: is far from being trivial.

Reed Maxwell 3/4/2015 7:55 AM

Deleted: good (

Reed Maxwell 3/4/2015 7:55 AM

Deleted:)

268 decreased and removed entirely as simulation time progressed. Large time steps (10,000h) were
269 used initially and were decreased (to 1h) as the stream network formed and overland flow
270 became more pronounced with reduced dampening. The entire simulation utilized
271 approximately 2.5M core hours of compute time, which resulted in less than 1 week of wall-
272 clock time (approximately 150 hours) given the large core counts and batch submission process.

273 Model results were compared to available observations of streamflow and hydraulic head
274 (the sum of pressure head and gravitational potential). Observed streamflow values were
275 extracted from a spatial dataset of current and historical U.S. Geological Survey (USGS) stream
276 gages mapped to the National Hydrography Dataset (NHD) (Stewart et al., 2006). The entire
277 dataset includes roughly 23,000 stations, of which just over half (13,567) fall within the CONUS
278 domain. For each station, the dataset includes location, drainage area, sampling time period and
279 flow characteristics including minimum, maximum, mean and a range of percentiles (1, 5, 10,
280 20, 25, 50, 75, 80, 90, 95, 99) compiled from the USGS gage records. For comparison, stations
281 without a reported drainage area, stations not located on or adjacent to a river cell in ParFlow,
282 and stations whose drainage area were not within twenty percent of the calculated ParFlow
283 drainage area were filtered out. This resulted in 4,736 stations for comparison. The 50th
284 percentile values for these stations are shown in Figure 2a. Note that these observations are not
285 naturalized, i.e. no attempt is made to remove dams and diversions along these streams and
286 rivers, however some of these effects will be minimized given the longer temporal averages.
287 Hydraulic head observations of groundwater at more than 160,000 locations were assembled by
288 Fan et al. (Fan et al. 2007; Fan et al. 2013). Figure 2b plots the corresponding water table depth
289 at each location calculated as the difference between elevation and hydraulic head. Note that

Reed Maxwell 3/4/2015 7:55 AM
Deleted: checked for plausibility against

291 these observations include groundwater pumping (most wells are drilled for extraction rather
292 than purely observation).

293

294 **Results and Discussion**

295 Figures 3 and 4 plot simulated streamflow and water table depth, respectively, over much
296 of continental North America, both on a log scale for flow (Figure 3) and water table depth
297 (Figure 4). Figure 3 shows a complex stream network with flow rates spanning many orders of
298 magnitude. Surface flows originate in the headwaters (or recharge zones) creating tributaries that
299 join to form the major river systems in North America. Note, as discussed previously that the
300 locations for flowing streams are not enforced in ParFlow but form due to ponded water at the
301 surface (i.e. values of $h>0$ in the top layer of the model in Equations 1-3). Overland flow is
302 promoted both by topographic convergence, and surface and subsurface flux; however, with this
303 formulation there is no requirement that all potential streams support flow. Thus, the model
304 captures the generation of the complete stream network without specifying the presence and
305 location of rivers in advance, but rather by allowing channelized flow to evolve as a result of
306 explicitly simulated non-linear physical processes.

307 The insets in Figure 3 demonstrate multiscale detail ranging from the continental river
308 systems to the first-order headwaters. In Figure 4, water table depth also varies over five orders
309 of magnitude. Whereas aridity drives large-scale differences in water table depth (Figure 1d), at
310 smaller scales, lateral surface and subsurface flow processes clearly dominate recharge and
311 subsurface heterogeneity (see insets to Figure 4). Water tables are deeper in the more arid
312 western regions, and shallower in the more humid eastern regions of the model. However, areas
313 of shallow water table exist along arid river channels and water table depths greater than 10m

314 exist in more humid regions. Note that this is a pre-development simulation, thus, results do not
315 include any anthropogenic water management features such as groundwater pumping, surface
316 water reservoirs, irrigation or urbanization—all of which are present in the observations. Many
317 of these anthropogenic impacts have been implemented into the ParFlow modeling framework
318 (Ferguson and Maxwell 2011; Condon and Maxwell 2013; Condon and Maxwell 2014).

319 ~~Although~~ anthropogenic impacts ~~clearly influence~~ water resources, a baseline simulation allows
320 for a comparison between the altered and unaltered systems in future ~~work~~.

321 Next we compare the results of the numerical experiment to observations. As noted
322 previously, this is not a calibrated model. Therefore, the purpose of these comparisons is to
323 ~~evaluate~~ model behavior and physical processes ~~against observations not to generate input~~

324 ~~parameters~~. Figure 5 plots observed and simulated hydraulic head and streamflow for the dataset
325 shown in Figure 2. Hydraulic head (Figure 5a) is plotted (as opposed to water table depth) as it
326 is the motivating force for lateral flow in the simulation; it includes both the topography and
327 pressure influences on the final solution. We see a very close agreement between observations
328 and model simulations, though given the large range in hydraulic heads the goodness of fit may
329 be ~~influenced~~ by ~~topography~~. Additional metrics and comparisons are explored below.

330 Simulated streamflow (Figure 5b) also agrees closely with observations. There is some bias,
331 particularly for smaller flows (which we emphasize by plotting in log scale), which also exhibit
332 more scatter than larger flows, and are likely due to the 1km grid resolution employed here.
333 Larger flows are more integrated measures of the system and might be less sensitive to resolution
334 or local heterogeneity in model parameters. We see this when linear least squared statistics are
335 computed where the R^2 value increases to 0.8.

Reed Maxwell 3/4/2015 7:55 AM

Deleted: While

Reed Maxwell 3/4/2015 7:55 AM

Deleted: are

Reed Maxwell 3/4/2015 7:55 AM

Deleted: influential on

Reed Maxwell 3/4/2015 7:55 AM

Deleted: provide a plausibility check of

Reed Maxwell 3/4/2015 7:55 AM

Deleted: .

Reed Maxwell 3/4/2015 7:55 AM

Deleted: somewhat driven

Reed Maxwell 3/4/2015 7:55 AM

Deleted: the underlying

343 Figure 6 plots histograms of predicted and observed water table depth (a), hydraulic head
344 (b), median (50th percentile) flow and 75th percentile flows (c-d). The hydraulic head shows
345 good agreement between simulated and observed (Figure 6b). While hydraulic head is the
346 motivation for lateral flow and has been used in prior comparisons (e.g. Fan et al 2007) both
347 observed and simulated values are highly dependent on the local elevation. Figure 6a plots the
348 water table depth below ground surface, or the difference between local elevation and
349 groundwater. Here we see the simulated water table depths are shallower than the observed,
350 something observed in prior simulations of large-scale water table depth (Fan et al 2013). The
351 observed water tables may include anthropogenic impacts, namely groundwater pumping, while
352 the model simulations do not and this is a likely cause for this difference. Also, because
353 groundwater wells are usually installed for extraction purposes there is no guarantee that the
354 groundwater observations are an unbiased sample of the system as a whole. Figure 6c plots the
355 steady-state derived flow values compared to median observed flow values and Figure 6d plots
356 these same steady-state simulated flows compared to the 75th percentile of the observed transient
357 flow at each station. While the ParFlow model provides a robust representation of runoff
358 generation processes, the steady-state simulations average event flows. We see the model
359 predicts greater flow than the 50th percentile observed flows (Figure 6c) and good agreement
360 between the model simulations and the 75th percentile observed flows (Figure 6d). This
361 indicates a potentially wet bias in the forcing, which might also explain the shallower water table
362 depths.

363 Figures 7 and 8 compare observed and simulated flows and water table depths for each of
364 the major basin encompassed by the model. Water tables are generally predicted to be shallower
365 in the model than observations with the exception of the Upper and Lower Colorado which

366 demonstrate better agreement between model simulations and observations than other basins.
367 These histograms agree with a visual inspection of Figures 2b and 4 which also indicate deeper
368 observed water tables. Figure 8 indicates that simulated histograms of streamflow also predict
369 more flow than the observations. This might indicate that the P-E forcing is too wet. However,
370 a comparison of streamflow for the Colorado Watershed, where water table depths agree (Figure
371 8 e and g) and flows are overpredicted (Figure 7 e and g), indicates a more complex set of
372 interactions than basic water balance driven by forcing.

373 To better diagnose model processes, model inputs are compared with model simulation
374 outputs over example regions chosen to isolate the impact of topographic slope, forcing and
375 hydraulic conductivity on subsurface-surface water hydrodynamics. We do this as a check to see
376 if and how this numerical experiment compares to real observations. It is important to use a
377 range of measures of success that might be different from that used in a model calibration where
378 inadequacies in model parameters and process might be muted while tuning the model to better
379 match observations. Figure 9 juxtaposes slope, potential recharge, surface flow, water table
380 depth, hydraulic conductivity and a satellite image composite also at 1km resolution (the NASA
381 Blue Marble image, (Justice et al. 2002)) and facilitates a visual diagnosis of control by the three
382 primary model inputs. While the model was run to steady-state and ultimately all the potential
383 recharge has to exit the domain as discharge, the distribution and partitioning between
384 groundwater and streams depends on the slope and hydraulic conductivity. Likewise, while
385 topographic lows create the potential for flow convergence, it is not a model requirement that
386 these will develop into stream loci. Figure 9 demonstrates some of these relationships quite
387 clearly over a portion of the model that transitions from semi-arid to more humid conditions as
388 the North and South Platte River systems join the Missouri. As expected changes in slope yield

389 flow convergence, however, this figure also shows that as recharge increases from west to east
390 ($X > 1700$ km, panel c) the model generally predicts shallower water tables and greater stream
391 density (panels d and e, respectively). Conversely, in localized areas of decreased P-E (e.g. 700
392 $< Y < 900$ km specifically south of the Platte River) water tables increase and stream densities
393 decrease. The satellite image (panel f) shows increases in vegetation that correspond to
394 shallower water tables and increased stream density.

395 Hydraulic conductivity also has a significant impact on water table depth and stream
396 network density. In areas of greater recharge in the eastern portion of Figure 9c, regions with
397 larger hydraulic conductivity (panel b) show decreased stream network density and increased
398 water table depths. This is more clearly demonstrated in Figure 10 (a region in the upper
399 Missouri) where, except for the northeast corner, recharge is uniformly low. Slopes are also
400 generally low (panel a), yet hydraulic conductivities show a substantial increase due to a change
401 in datasets between state and country boundaries (panel b, $X > 1250$ km, $Y > 1400$ km). The
402 relative increase in hydraulic conductivity decreases hydraulic gradients under steady state
403 conditions and generally increases water table depth, which in turn decreases stream network
404 density. This change in hydraulic conductivity yields a decrease in the formation of stream
405 networks resulting in an increase in water table depth. Thus, hydraulic conductivity has an
406 important role in partitioning moisture between surface and subsurface flow, also under steady-
407 state conditions. While mass balance requires that overall flow must be conserved, larger
408 conductivity values allow this flow to be maintained within the subsurface while lower
409 conductivities force the surface stream network to maintain this flow. In turn, stream networks
410 connect regions of varying hydrodynamic conditions and may result in locally infiltrating
411 conditions creating a losing-stream to recharge groundwater. This underscores the connection

412 between input variables and model predictions, an equal importance of hydraulic conductivity to
413 recharge in model states and the need to continually improve input datasets.

414 Finally, the connection between stream flow and drainage area is a classical scaling
415 relationship (Rodriguez-Iturbe and Rinaldo 2001), which usually takes the power law form
416 $Q=kA^n$, where Q is volumetric streamflow [L^3T^{-1}], A is the contributing upstream area [L^2] and k
417 [LT^{-1}] and n are empirical constants. While this relationship has been demonstrated for
418 individual basins and certain flow conditions (Rodriguez-Iturbe and Rinaldo 2001), generality
419 has not been established (Glaster 2009). Figure 11a plots simulated streamflow as a function of
420 associated drainage area on log-log axes, and Figure 11b plots the same variables for median
421 observed streamflow from more than 4,000 gaging stations. While no single functional
422 relationship is evident from this plot, there is a striking maximum limit of flow as a function of
423 drainage area with a continental scaling coefficient of $n = 0.84$. Both Figures 11a and b are
424 colored by aridity index (AI), the degree of dryness of a given location. Color gradients that
425 transition from blue (more humid) to red (more arid) show that humid basins fall along the
426 maximum flow-discharge line, while arid basins have less discharge and fall below this line. For
427 discharge observations (Figure 11b) the same behavior is observed, where more humid stations
428 fall along the $n=0.9$ line and more arid stations fall below this line. Essentially this means that in
429 humid locations, where water is not a limiting factor, streamflow scales most strongly with
430 topography and area. Conversely arid locations fall below this line because flow to streams is
431 limited by groundwater storage.

432 The model presented here represents a first, high-resolution integrated simulation over
433 continental-scale river basins in North America using the best available data. However, primary
434 input datasets are used (potential recharge, subsurface properties and topography), which clearly

435 require improvement. For example, higher resolution simulations are feasible, given that the
436 ParFlow model exhibits better than 80% parallel efficiency for more than 8 billion compute cells.
437 This could improve the surface and subsurface prediction; although, we do not expect the form
438 of the scaling relationships as shown in Figure 11 to change with an increase in resolution.
439 Higher resolution simulations would require higher resolution parameter fields that do not exist
440 at this time. Similarly, model lower boundaries (i.e. the overall thickness of the subsurface)
441 could be extended given information about deeper hydrogeologic formations and their properties.
442 The model domain could be expanded to larger spatial extent, either over more of continental
443 North America, coastlines, or even globally. Thus, the study strongly motivates improved,
444 unified input and validation data sets for integrated hydrologic models at the continental scale,
445 similar to data products available to the atmospheric sciences.

446 **Conclusions**

447 Here we present the results of an integrated, multiphysics-based hydrologic simulation
448 covering much of Continental North America at hyperresolution (1km). This numerical
449 experiment provides a consistent theoretical framework for the analysis of groundwater and
450 surface water interactions and scaling from the headwaters to continental scale (10^0 - 10^7 km²).
451 The framework exploits high performance computing to meet this grand challenge in hydrology
452 (Wood et al. 2011; Gleeson and Cardiff 2014; Bierkens et al. 2015). We demonstrate that
453 continental-scale, integrated hydrologic models are feasible and can reproduce observations and
454 the essential features of streamflow and groundwater. Results show that scaling of surface flow
455 is related to both drainage area and aridity. These results may be interrogated further to
456 understand the role of topography, subsurface properties and climate on groundwater table and

457 streamflow, and used as a platform to diagnose scaling behavior, e.g. surface flow from the
458 headwaters to the continent.

459 These presented results are a first-step in high resolution, integrated, continental-scale
460 simulation. We simulate an unaltered, or pre-development scenario of groundwater and surface
461 water flows under steady-state conditions. As such, the discussion focuses on the physical
462 controls of groundwater surface water interactions and scaling behavior; however there are
463 obvious limitations to this scenario and these simulations. Clearly reservoir management,
464 groundwater pumping, irrigation, diversion and urban expansion all shape modern hydrology.
465 Work has been undertaken to include these features within the ParFlow framework at smaller
466 scales (Ferguson and Maxwell 2011; Ferguson and Maxwell 2012; Condon and Maxwell 2013;
467 Condon and Maxwell 2014) and an important next step is to scale the impacts out to the
468 continent.

469 Additionally, the steady-state simulation does not take into consideration temporal
470 dynamics or complex land-surface processes, also important in determining the quantity and
471 fluxes of water. These limitations can all be addressed within the current modeling framework
472 but require transient simulations and additional computational resources. Model performance is
473 also limited by the quality of available input datasets. As noted throughout the discussion,
474 existing datasets are subject to uncertainty and are clearly imperfect. As improved subsurface
475 characterization becomes available, this information can be used to better inform models and
476 fully understand the propagation of uncertainty in these types of numerical experiments (e.g.
477 Maxwell and Kollet 2008; Kollet 2009). However, while the magnitudes of states and fluxes may
478 change with improved datasets, the overall trends and responses predicted here are not likely to
479 change. While there are always improvements to be made, these simulations represent a critical

Reed Maxwell 3/4/2015 7:55 AM

Deleted:

Reed Maxwell 3/4/2015 7:55 AM

Deleted: within the confines of the numerical experiment.

483 first step in understanding coupled surface subsurface hydrologic processes and scaling at
484 continental scales resolving variances over four for orders of spatial scales.

485 This study highlights the utility of high performance computing in addressing the grand
486 challenges in hydrological sciences and represents an important advancement in our
487 understanding of hydrologic scaling in continental river basins. By providing an integrated
488 model we open up a useful avenue of research to bridge physical processes across spatial scales
489 in a hydrodynamic, physics-based upscaling framework.

490

491 **Code Availability**

492 ParFlow is an open-source, modular, parallel integrated hydrologic platform freely available via
493 the GNU LGPL license agreement. ParFlow is developed by a community led by the Colorado
494 School of Mines and F-Z Jülich with contributors from a number of other institutions. Specific
495 versions of ParFlow are archived with complete documentation and may be downloaded¹ or
496 checked-out from a commercially hosted, free SVN repository; v3, r693 was the version used in
497 this study. The input data and simulations presented here will be made available and may be
498 obtained by contacting the lead author via email.

499

¹ http://inside.mines.edu/~rmaxwell/maxwell_software.shtml

500

501 **Figures**

502

503 Figure 1. Maps of top soil type (applied over the top 2 m of the model) (a), elevation (masl) (b),

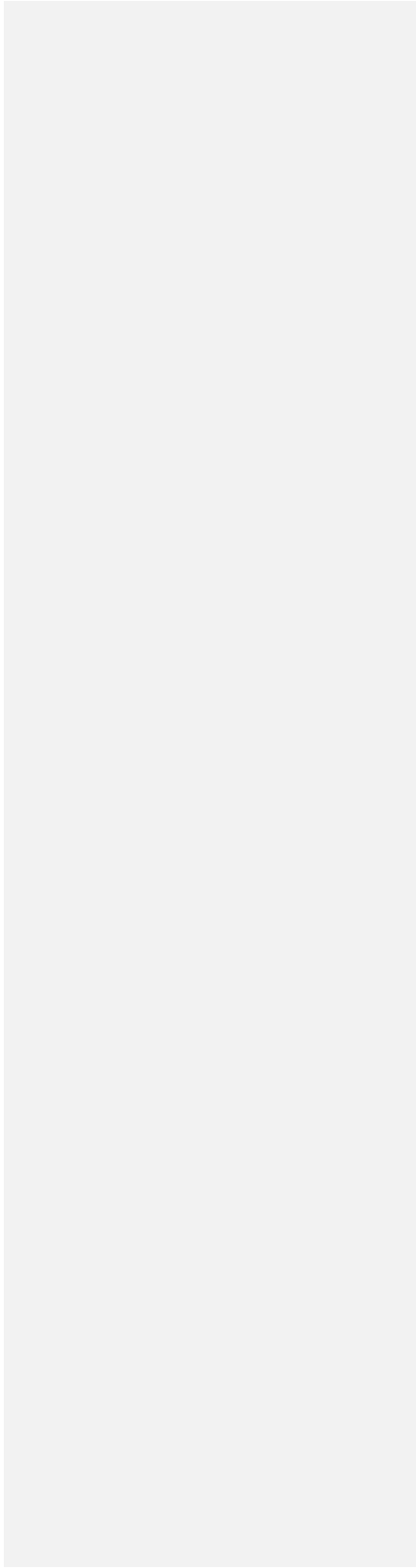
504 bottom soil type (c), potential recharge, P-E, (m/y) (d), saturated hydraulic conductivity (m/h_s)

505 applied over the bottom 100 m of the model) (e) over the model domain (f).

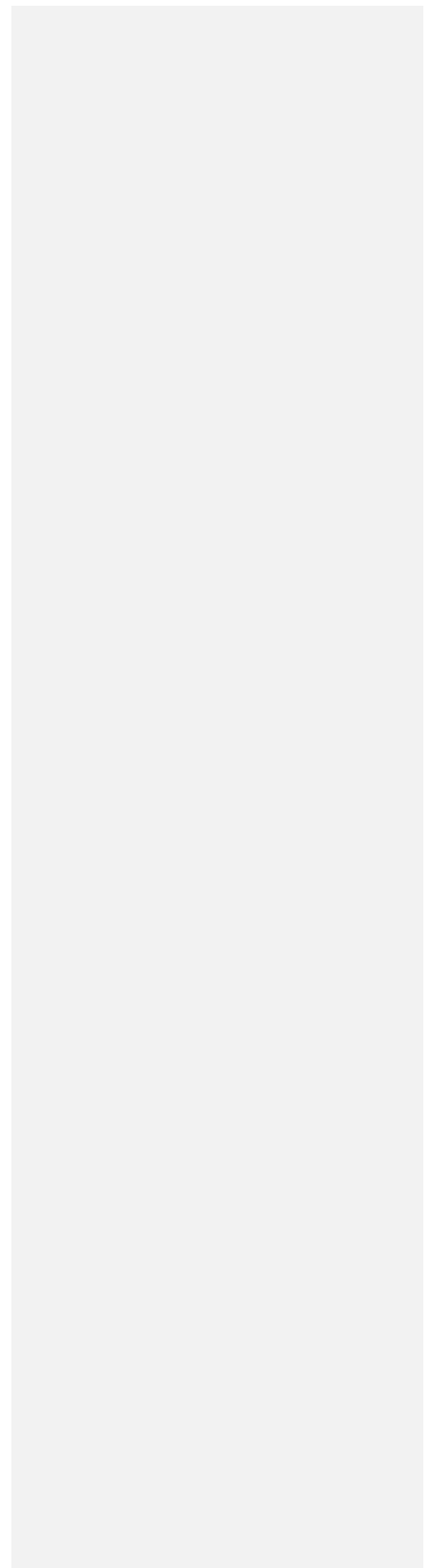
506

507
508
509

Figure 2. Plot of observed streamflow (a) and observed water table depth (b).

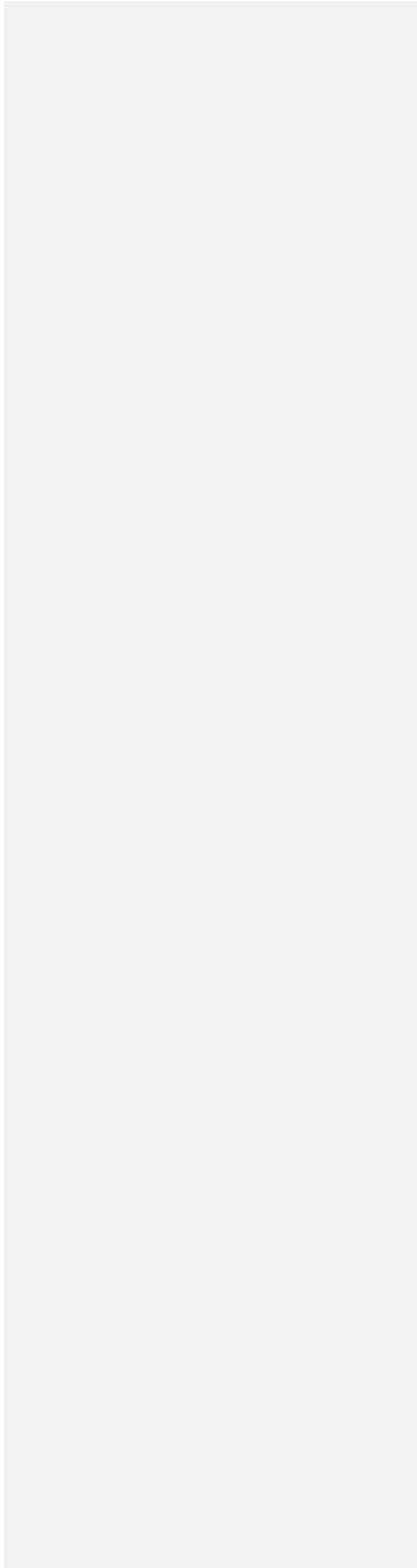


510
511 Figure 3. Map of simulated surface flow (m^3/s) over the CONUS domain with two insets
512 zooming into the Ohio river basin. Colors represent surface flow in log scale and line widths
513 vary slightly with flow for the first two panels.
514



515
516
517
518
519

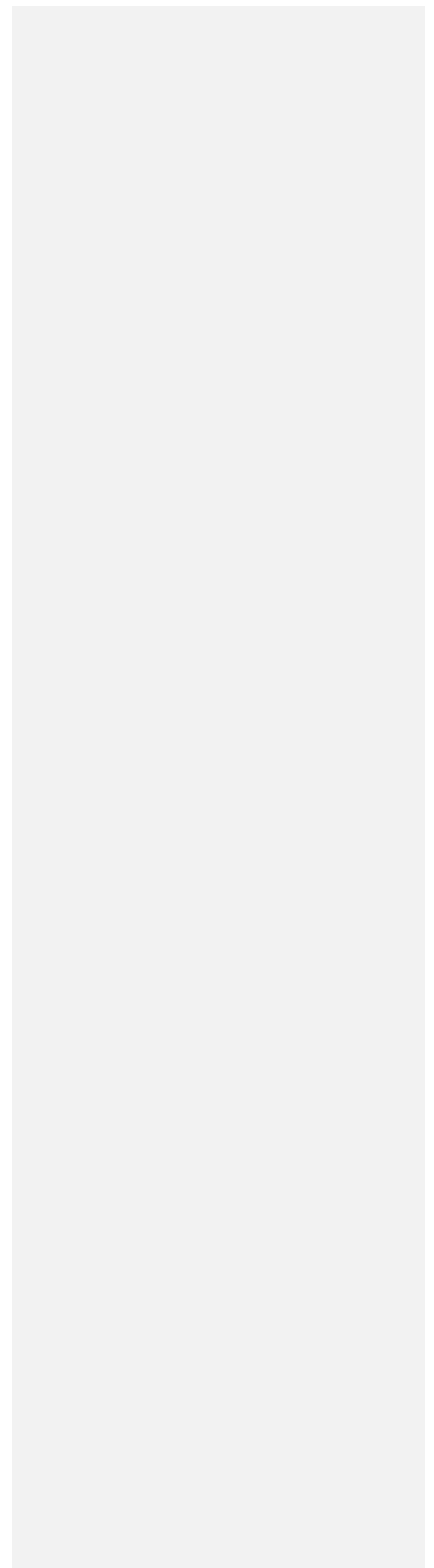
Figure 4. Map of water table depth (m) over the simulation domain with two insets zooming into the North and South Platte River basin, headwaters to the Mississippi. Colors represent depth in log scale (from 0.01 to 100m).



520

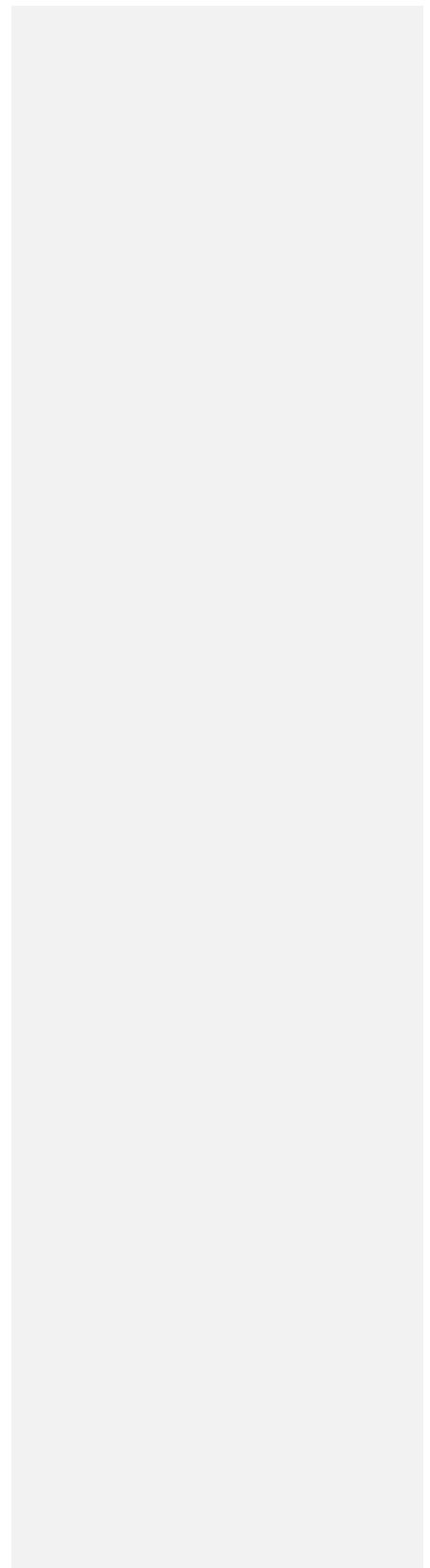
521 Figure 5. Scatterplots of simulated v. observed hydraulic head (a) and surface flow (b).

522



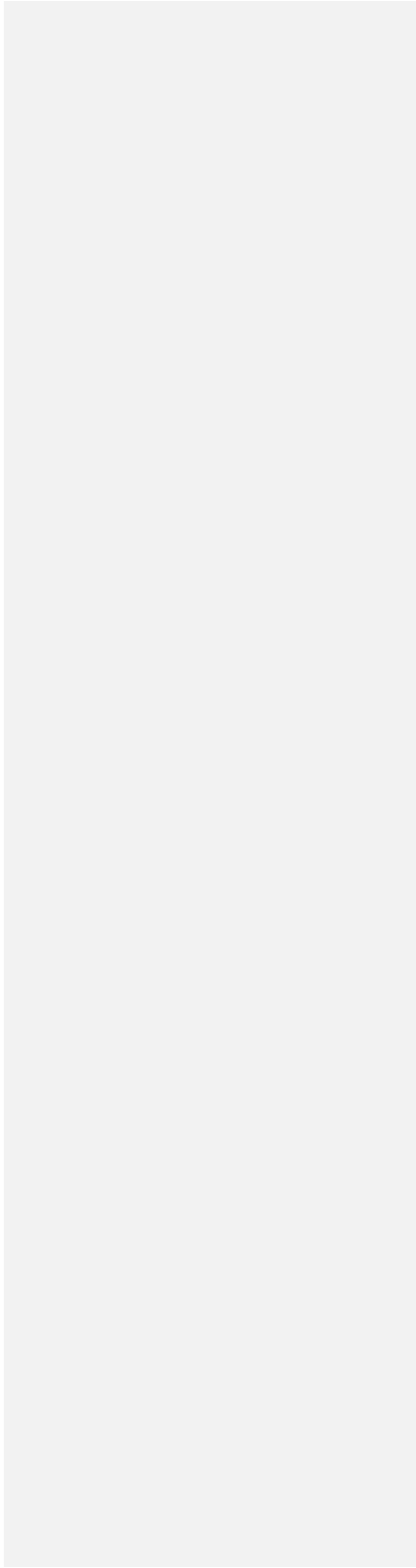
523
524
525
526

Figure 6. Histograms of simulated and observed water table depth (a), hydraulic head (b), median observed flow (c) and 75th percentile observed flow (d).



527
528
529
530
531

Figure 7. Distributions of observed and simulated streamflow by basin as indicated.



532
533
534
535
536
537
538
539
540
541
542
543
544
545
546
547
548
549
550

Figure 8. Distributions of observed and simulated water table depth by basin as indicated.

Figure 9. Plots of topographic slope (a), hydraulic conductivity (b) potential recharge (c), water table depth (d), streamflow (e) and satellite image (f) for a region of the model covering the Platte River basin.

Figure 10. Plots of topographic slope (a), hydraulic conductivity (b) potential recharge (c), water table depth (d), streamflow (e) and satellite image (f) for a region of the model covering the Upper Missouri basin.

Figure 11. Plots of scaling relationships for simulated and median observed surface flow. Log-scale plots of surface flow as a function of contributing drainage area derived from the model simulation (a) and observations (b). Individual symbols are colored by aridity index (AI) with blue colors being humid and red colors being arid in panels (a) and (b).

551
552
553
554
555
556
557
558
559
560
561
562
563
564
565
566
567
568
569
570
571
572
573
574
575
576
577
578
579
580
581
582
583
584
585
586
587
588
589
590
591
592
593
594
595

References

- Anyah, R. O., C. P. Weaver, G. Miguez-Macho, Y. Fan and A. Robock (2008). "Incorporating water table dynamics in climate modeling: 3. Simulated groundwater influence on coupled land-atmosphere variability." Journal of Geophysical Research-Atmospheres **113**(D7): 15,
- Ashby, S. F. and R. D. Falgout (1996). "A parallel multigrid preconditioned conjugate gradient algorithm for groundwater flow simulations." Nuclear Science and Engineering **124**(1): 145-159,
- Beven, K. (2004). "Robert e. Horton's perceptual model of infiltration processes." Hydrological Processes **18**(17): 3447-3460,
- Bierkens, M. F. P., V. A. Bell, P. Burek, N. Chaney, L. E. Condon, C. H. David, A. de Roo, P. Döll, N. Drost, J. S. Famiglietti, M. Flörke, D. J. Gochis, P. Houser, R. Hut, J. Keune, S. Kollet, R. M. Maxwell, J. T. Reager, L. Samaniego, E. Sudicky, E. H. Sutanudjaja, N. van de Giesen, H. Winsemius and E. F. Wood (2015). "Hyper-resolution global hydrological modelling: What is next?" Hydrological Processes **29**(2): 310-320, 10.1002/hyp.10391
- Camporese, M., C. Paniconi, M. Putti and S. Orlandini (2010). "Surface-subsurface flow modeling with path-based runoff routing, boundary condition-based coupling, and assimilation of multisource observation data." Water Resources Research **46**(2): W02512, 10.1029/2008wr007536
- Camporese, M., C. Paniconi, M. Putti and S. Orlandini (2010). "Surface-subsurface flow modeling with path-based runoff routing, boundary condition-based coupling, and assimilation of multisource observation data." Water Resour. Res. **46**(2): W02512, doi: 10.1029/2008wr007536
- Camporese, M., D. Penna, M. Borgia and C. Paniconi (2014). "A field and modeling study of nonlinear storage-discharge dynamics for an alpine headwater catchment." Water Resources Research **50**(2): 806-822, 10.1002/2013wr013604
- Condon, L. E. and R. M. Maxwell (2013). "Implementation of a linear optimization water allocation algorithm into a fully integrated physical hydrology model." Advances in Water Resources **60**(0): 135-147, <http://dx.doi.org/10.1016/j.advwatres.2013.07.012>
- Condon, L. E. and R. M. Maxwell (2014). "Feedbacks between managed irrigation and water availability: Diagnosing temporal and spatial patterns using an integrated hydrologic model." Water Resources Research **50**(3): 2600-2616, 10.1002/2013wr014868
- Condon, L. E., R. M. Maxwell and S. Gangopadhyay (2013). "The impact of subsurface conceptualization on land energy fluxes." Advances in Water Resources **60**(0): 188-203, <http://dx.doi.org/10.1016/j.advwatres.2013.08.001>
- Döll, P., H. Hoffmann-Dobrev, F. T. Portmann, S. Siebert, A. Eicker, M. Rodell, G. Strassberg and B. R. Scanlon (2012). "Impact of water withdrawals from groundwater and surface water on continental water storage variations." - **59**, **Äi60**(- 0): - 156,
- Dunne, T. (1983). "Relation of field studies and modeling in the prediction of storm runoff." Journal of Hydrology **65**(1, Äi3): 25-48, [http://dx.doi.org/10.1016/0022-1694\(83\)90209-3](http://dx.doi.org/10.1016/0022-1694(83)90209-3)
- Fan, Y., H. Li and G. Miguez-Macho (2013). "Global patterns of groundwater table depth." Science **339**(6122): 940-943, 10.1126/science.1229881

596 Fan, Y., G. Miguez-Macho, C. P. Weaver, R. Walko and A. Robock (2007). "Incorporating
597 water table dynamics in climate modeling: 1. Water table observations and equilibrium
598 water table simulations." *Journal of Geophysical Research-Atmospheres* **112**(D10): -,
599 Ferguson, I. M. and R. M. Maxwell (2011). "Hydrologic and land-energy feedbacks of
600 agricultural water management practices." *Environmental Research Letters* - **6**(- 1),
601 doi:10.1088/1748-9326/6/1/014006

602 Ferguson, I. M. and R. M. Maxwell (2012). "Human impacts on terrestrial hydrology: Climate
603 change versus pumping and irrigation." *Environmental Research Letters* **7**(4): 044022,
604 Freeze, R. A. and R. L. Harlan (1969). "Blueprint for a physically-based, digitally-simulated
605 hydrologic response model." *Journal of Hydrology* **9**: 237-258,
606 Glaster, J. C. (2009). "Testing the linear relationship between peak annual river discharge and
607 drainage area using long-term usgs river gauging records." *Geological Society of
608 America Special Papers* **451**: 159-171, 10.1130/2009.2451(11)

609 Gleeson, T. and M. Cardiff (2014). "The return of groundwater quantity: A mega-scale and
610 interdisciplinary "future of hydrogeology"?" *Hydrogeology Journal*: **4**, 10.1007/s10040-
611 013-0998-8

612 Gleeson, T., L. Marklund, L. Smith and A. H. Manning (2011). "Classifying the water table at
613 regional to continental scales." *Geophysical Research Letters* **38**(L05401): 6,
614 10.1029/2010GL046427

615 Gleeson, T., L. Smith, N. Moosdorf, J. Hartmann, H. H. Dürr, A. H. Manning, L. P. H. van Beek
616 and A. M. Jellinek (2011). "Mapping permeability over the surface of the earth."
617 *Geophysical Research Letters* **38**(2): L02401, 10.1029/2010gl045565

618 Goderniaux, P., S. Brouyère, H. J. Fowler, S. Blenkinsop, R. Therrien, P. Orban and A.
619 Dassargues (2009). "Large scale surface, subsurface hydrological model to assess
620 climate change impacts on groundwater reserves." *Journal of Hydrology* **373**(1, 2):
621 122-138, <http://dx.doi.org/10.1016/j.jhydrol.2009.04.017>

622 Horton, R. E. (1933). "The role of infiltration in the hydrologic cycle." *Transactions-American
623 Geophysical Union* **14**: 446-460,
624 Jiang, X., G. Y. Niu and Z. L. Yang (2009). "Impacts of vegetation and groundwater dynamics
625 on warm season precipitation over the central united states." *Journal of Geophysical
626 Research* **114**: 15,
627 Jones, J. E. and C. S. Woodward (2001). "Newton-krylov-multigrid solvers for large-scale,
628 highly heterogeneous, variably saturated flow problems." *Advances in Water Resources*
629 **24**(7): 763-774,
630 Jones, J. P., E. A. Sudicky, A. E. Brookfield and Y. J. Park (2006). "An assessment of the tracer-
631 based approach to quantifying groundwater contributions to streamflow." *Water Resour.
632 Res.* **42**, 10.1029/2005wr004130

633 Jones, J. P., E. A. Sudicky and R. G. McLaren (2008). "Application of a fully-integrated surface-
634 subsurface flow model at the watershed-scale: A case study." *Water Resources Research*
635 **44**(3): W03407, 10.1029/2006wr005603

636 Justice, C. O., J. R. G. Townshend, E. F. Vermote, E. Masuoka, R. E. Wolfe, N. Saleous, D. P.
637 Roy and J. T. Morisette (2002). "An overview of modis land data processing and product
638 status." *Remote Sensing of Environment* **83**(1, 2): 3-15,
639 [http://dx.doi.org/10.1016/S0034-4257\(02\)00084-6](http://dx.doi.org/10.1016/S0034-4257(02)00084-6)

640 Kirkby, M. (1988). "Hillslope runoff processes and models." *Journal of Hydrology* **100**(1, 3):
641 315-339, [http://dx.doi.org/10.1016/0022-1694\(88\)90190-4](http://dx.doi.org/10.1016/0022-1694(88)90190-4)

642 Kollet, S. J. (2009). "Influence of soil heterogeneity on evapotranspiration under shallow water
643 table conditions: Transient, stochastic simulations." Environmental Research Letters **4**(3):
644 9,
645 Kollet, S. J., I. Cvijanovic, D. Schüttemeyer, R. M. Maxwell, A. F. Moene and B. P. (2009).
646 "The influence of rain sensible heat, subsurface heat convection and the lower
647 temperature boundary condition on the energy balance at the land surface." Vadose Zone
648 Journal **8**(4): 12,
649 Kollet, S. J. and R. M. Maxwell (2006). "Integrated surface-groundwater flow modeling: A free-
650 surface overland flow boundary condition in a parallel groundwater flow model."
651 Advances in Water Resources **29**(7): 945-958,
652 Kollet, S. J. and R. M. Maxwell (2008). "Capturing the influence of groundwater dynamics on
653 land surface processes using an integrated, distributed watershed model." Water
654 Resources Research **44**(W02402): 18, doi:10.1029/2007WR006004
655 Kollet, S. J., R. M. Maxwell, C. S. Woodward, S. Smith, J. Vanderborght, H. Vereecken and C.
656 Simmer (2010). "Proof of concept of regional scale hydrologic simulations at hydrologic
657 resolution utilizing massively parallel computer resources." Water Resources Research
658 **46**(W04201): -, Doi 10.1029/2009wr008730
659 Krakauer, N. Y., H. Li and Y. Fan (2014). "Groundwater flow across spatial scales: Importance
660 for climate modeling." Environmental Research Letters **9**(3): 034003,
661 Kumar, M., C. J. Duffy and K. M. Salvage (2009). "A second order accurate, finite volume
662 based, integrated hydrologic modeling (film) framework for simulation of surface and
663 subsurface flow." Vadose Zone Journal,
664 Maurer, E. P., A. W. Wood, J. C. Adam, D. P. Lettenmaier and B. Nijssen (2002). "A long-term
665 hydrologically based dataset of land surface fluxes and states for the conterminous united
666 states*." Journal of Climate **15**(22): 3237-3251, 10.1175/1520-
667 0442(2002)015<3237:althbd>2.0.co;2
668 Maxwell, R. M. (2013). "A terrain-following grid transform and preconditioner for parallel,
669 large-scale, integrated hydrologic modeling." Advances in Water Resources **53**: 109-117,
670 <http://dx.doi.org/10.1016/j.advwatres.2012.10.001>
671 Maxwell, R. M., F. K. Chow and S. J. Kollet (2007). "The groundwater-land-surface-atmosphere
672 connection: Soil moisture effects on the atmospheric boundary layer in fully-coupled
673 simulations." Advances in Water Resources **30**(12): 2447-2466, Doi
674 10.1016/J.Advwatres.2007.05.018
675 Maxwell, R. M. and S. J. Kollet (2008). "Interdependence of groundwater dynamics and land-
676 energy feedbacks under climate change." Nature Geosci **1**(10): 665-669,
677 Maxwell, R. M. and S. J. Kollet (2008). "Quantifying the effects of three-dimensional subsurface
678 heterogeneity on hortonian runoff processes using a coupled numerical, stochastic
679 approach." Advances in Water Resources **31**(5): 807-817,
680 Maxwell, R. M., J. D. Lundquist, J. D. Mirocha, S. G. Smith, C. S. Woodward and A. F. B.
681 Tompson (2011). "Development of a coupled groundwater-atmospheric model." Monthly
682 Weather Review doi: **10.1175/2010MWR3392**(139): 96-116,
683 Maxwell, R. M., M. Putti, S. Meyerhoff, J.-O. Delfs, I. M. Ferguson, V. Ivanov, J. Kim, O.
684 Kolditz, S. J. Kollet, M. Kumar, S. Lopez, J. Niu, C. Paniconi, Y.-J. Park, M. S.
685 Phanikumar, C. Shen, E. A. Sudicky and M. Sulis (2014). "Surface-subsurface model
686 intercomparison: A first set of benchmark results to diagnose integrated hydrology and
687 feedbacks." Water Resources Research **50**(2): 1531-1549, 10.1002/2013wr013725

688 Miguez-Macho, G., Y. Fan, C. P. Weaver, R. Walko and A. Robock (2007). "Incorporating
689 water table dynamics in climate modeling: 2. Formulation, validation, and soil moisture
690 simulation." *Journal of Geophysical Research-Atmospheres* **112**(D13): -,
691 Mikkelsen, K. M., R. M. Maxwell, I. Ferguson, J. D. Stednick, J. E. McCray and J. O. Sharp
692 (2013). "Mountain pine beetle infestation impacts: Modeling water and energy budgets at
693 the hill-slope scale." *Ecohydrology* **6**(1): 64-72, 10.1002/eco.278
694 Osei-Kuffuor, D., R. M. Maxwell and C. S. Woodward "Improved numerical solvers for implicit
695 coupling of subsurface and overland flow." *Advances in Water Resources*(0),
696 <http://dx.doi.org/10.1016/j.advwatres.2014.09.006>
697 Osei-Kuffuor, D., R. M. Maxwell and C. S. Woodward (2014). "Improved numerical solvers for
698 implicit coupling of subsurface and overland flow." *Advances in Water Resources* **74**(0):
699 185-195, <http://dx.doi.org/10.1016/j.advwatres.2014.09.006>
700 Qu, Y. and C. J. Duffy (2007). "A semidiscrete finite volume formulation for multiprocess
701 watershed simulation." *Water Resources Research* **43**(W08419): 18,
702 doi:10.1029/2006WR005752
703 Richards, L. A. (1931). "Capillary conduction of liquids in porous mediums." *Physics* **1**: 318-
704 333,
705 Rihani, J. F., R. M. Maxwell and F. K. Chow (2010). "Coupling groundwater and land surface
706 processes: Idealized simulations to identify effects of terrain and subsurface
707 heterogeneity on land surface energy fluxes." *Water Resour. Res.* **46**: 1-14,
708 doi:10.1029/2010WR009111
709 Rodell, M., I. Velicogna and J. S. Famiglietti (2009). "Satellite-based estimates of groundwater
710 depletion in india." *Nature* **460**(7258): 999-1002,
711 Rodriguez-Iturbe, I. and A. Rinaldo (2001). *Fractal river basins: Chance and self-organization*,
712 Cambridge University Press.
713 Schaap, M. G. and F. J. Leij (1998). "Database-related accuracy and uncertainty of pedotransfer
714 functions." *Soil Science* **163**(10): 765-779,
715 Shi, Y., K. J. Davis, C. J. Duffy and X. Yu (2013). "Development of a coupled land surface
716 hydrologic model and evaluation at a critical zone observatory." *Journal of*
717 *Hydrometeorology* **14**(5): 1401-1420, 10.1175/jhm-d-12-0145.1
718 Sudicky, E., J. Jones, Y.-J. Park, A. Brookfield and D. Colautti (2008). "Simulating complex
719 flow and transport dynamics in an integrated surface-subsurface modeling framework."
720 *Geosciences Journal* **12**(2): 107-122, 10.1007/s12303-008-0013-x
721 Sulis, M., C. Paniconi, M. Marrocu, D. Huard and D. Chaumont (2012). "Hydrologic response to
722 multimodel climate output using a physically based model of groundwater/surface water
723 interactions." *Water Resources Research* **48**(12): W12510, 10.1029/2012wr012304
724 Taylor, R. G., B. Scanlon, P. Doll, M. Rodell, R. van Beek, Y. Wada, L. Longuevergne, M.
725 Leblanc, J. S. Famiglietti, M. Edmunds, L. Konikow, T. R. Green, J. Chen, M. Taniguchi,
726 M. F. P. Bierkens, A. MacDonald, Y. Fan, R. M. Maxwell, Y. Yecheili, J. J. Gurdak, D.
727 M. Allen, M. Shamsudduha, K. Hiscock, P. J. F. Yeh, I. Holman and H. Treidel (2013).
728 "Ground water and climate change." *Nature Clim. Change* **3**(4): 322-329,
729 Therrien, R., E. Sudicky, Y. Park and R. McLaren (2012). *Hydrogeosphere: A three-dimensional*
730 *numerical modelling describing fully-*
731 *integrated subsurface and surface flow and transport. User guide. Waterloo, Ontario, Canada,*
732 *Aquanty Inc.*

733 van Genuchten, M. T. (1980). "A closed-form equation for predicting the hydraulic conductivity
734 of unsaturated soils." Soil Science Society of America Journal **44**(5): 892-898,
735 VanderKwaak, J. E. and K. Loague (2001). "Hydrologic-response simulations for the r-5
736 catchment with a comprehensive physics-based model." Water Resources Research
737 **37**(4): 999-1013,
738 Williams, J. L. and R. M. Maxwell (2011). "Propagating subsurface uncertainty to the
739 atmosphere using fully-coupled, stochastic simulations." Journal of Hydrometeorology,
740 doi:10.1175/2011JHM1363.1
741 Wood, B. D. (2009). "The role of scaling laws in upscaling." Advances in Water Resources
742 **32**(5): 723-736, <http://dx.doi.org/10.1016/j.advwatres.2008.08.015>
743 Wood, E. F., J. K. Roundy, T. J. Troy, L. P. H. van Beek, M. F. P. Bierkens, E. Blyth, A. de Roo,
744 P. Döll, M. Ek, J. Famiglietti, D. Gochis, N. van de Giesen, P. Houser, P. R. Jaffé, S.
745 Kollet, B. Lehner, D. P. Lettenmaier, C. Peters-Lidard, M. Sivapalan, J. Sheffield, A.
746 Wade and P. Whitehead (2011). "Hyperresolution global land surface modeling: Meeting
747 a grand challenge for monitoring earth's terrestrial water." Water Resources Research
748 **47**(5): W05301, 10.1029/2010wr010090
749 Xia, Y., K. Mitchell, M. Ek, B. Cosgrove, J. Sheffield, L. Luo, C. Alonge, H. Wei, J. Meng, B.
750 Livneh, Q. Duan and D. Lohmann (2012). "Continental-scale water and energy flux
751 analysis and validation for north american land data assimilation system project phase 2
752 (nldas-2): 2. Validation of model-simulated streamflow." Journal of Geophysical
753 Research: Atmospheres **117**(D3): D03110, 10.1029/2011jd016051
754
755